Electronic Supplementary Material (ESI) for Journal of Materials Chemistry A.

Supplementary Information

Nanochannel-confined charge repulsion of ions in a reduced graphene oxide membrane

Kecheng Guan, Shengyao Wang, Yufan Ji, Yuandong Jia, Lei Zhang, Kai Ushio, Yuqing Lin, Wanqin Jin, Hideto Matsuyama**

Table of contents

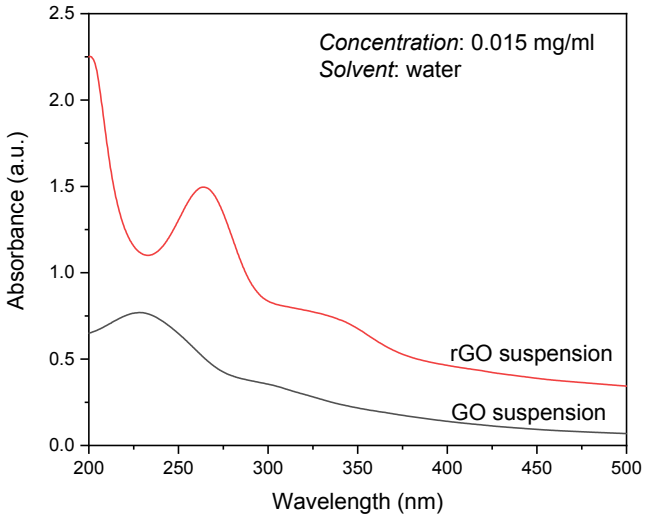

Figure S1 UV-vis spectra of GO and rGO suspensions.

After reduction, the intensity of the UV-vis absorption peaks for the rGO suspension was located at ~270 nm, with a red-shift from that of the GO suspension at ~230 nm. The overall increase in the absorption intensity in the spectrum of the rGO suspension also implied the restoration of the aromatic structure.

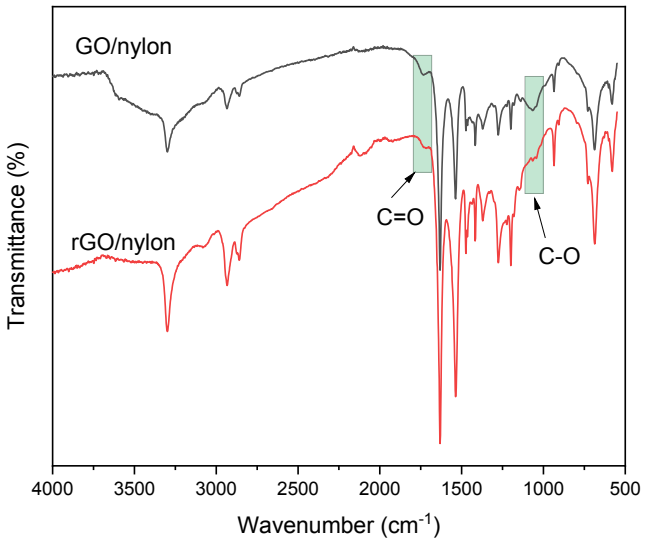

Figure S2 FTIR spectra of GO and rGO membranes supported on nylon filter membranes.

In comparison with the spectrum of GO, rGO displayed decreased peak intensities for the oxygenated functional groups such as carboxyl (C=O) and alkoxy (C-O) at ~1740, and ~1064 cm^{-1}, respectively.

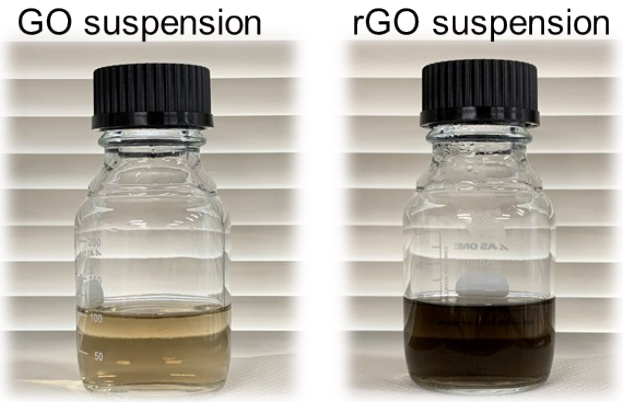

Figure S3 Digital photos of GO and rGO suspensions.

A larger quantity of rGO suspension could easily be obtained by scaling up the quantities of GO, L-AA, ammonia solution, and water solvent.

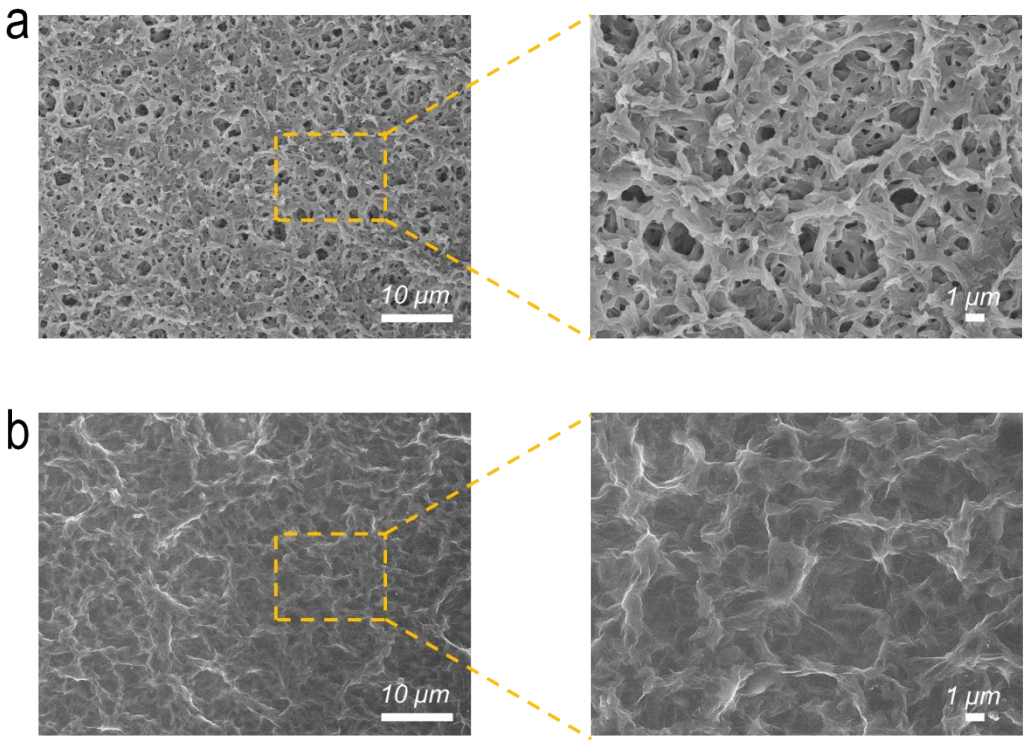

Figure S4 SEM images of a) a nylon membrane filter and b) nylon-supported rGO membranes.

The micro-roughness of the nylon membrane filter contributed to the firm adhesion of GO-based laminates by providing a sufficient contact area to the rGO layer.

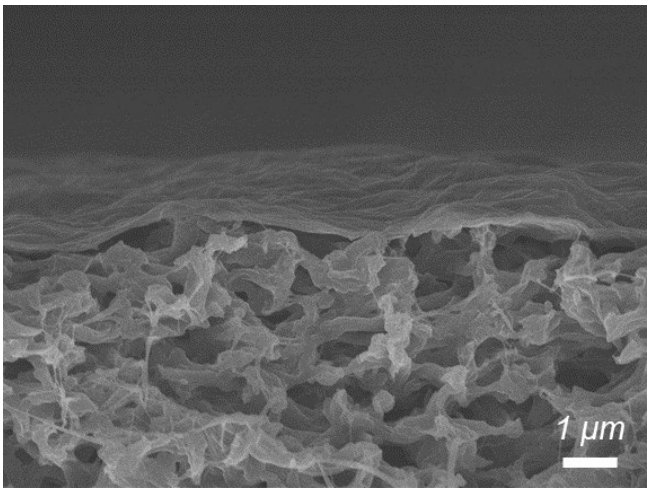

Figure S5 SEM image of a nylon-supported rGO membrane showing a cross-sectional structure view.

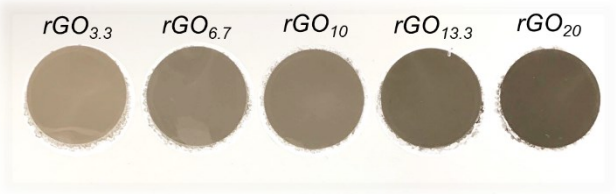

Figure S6 Digital photos of rGO membranes with different degrees of reduction. The subscripted numbers denote the weight ratios of L-AA to rGO.

The degree of reduction of the rGO membrane was controlled by the dosage of the reducing agent, L-AA.

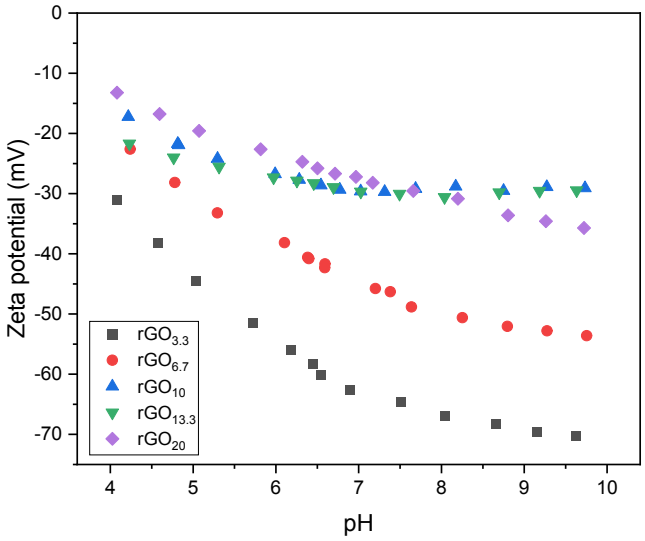

Figure S7 Zeta potential analysis of rGO membranes.

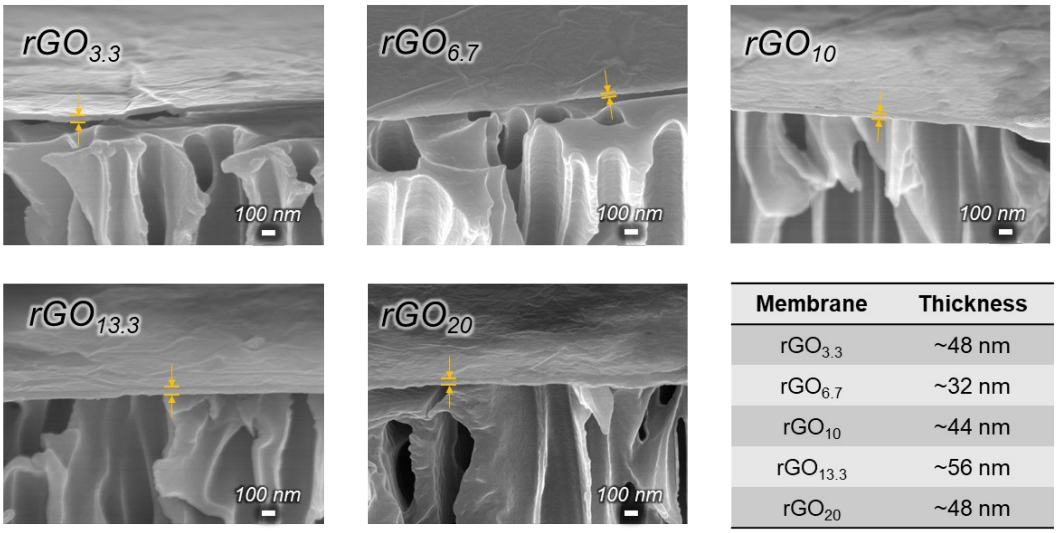

Membrane	Thickness
$rGO_{3.3}$	~48 nm
$rGO_{6.7}$	~32 nm
rGO_{10}	~44 nm
$rGO_{13.3}$	~56 nm
rGO_{20}	~48 nm

Figure S8 SEM images of PC membrane filter-supported rGO membranes showing cross-sectional structures.

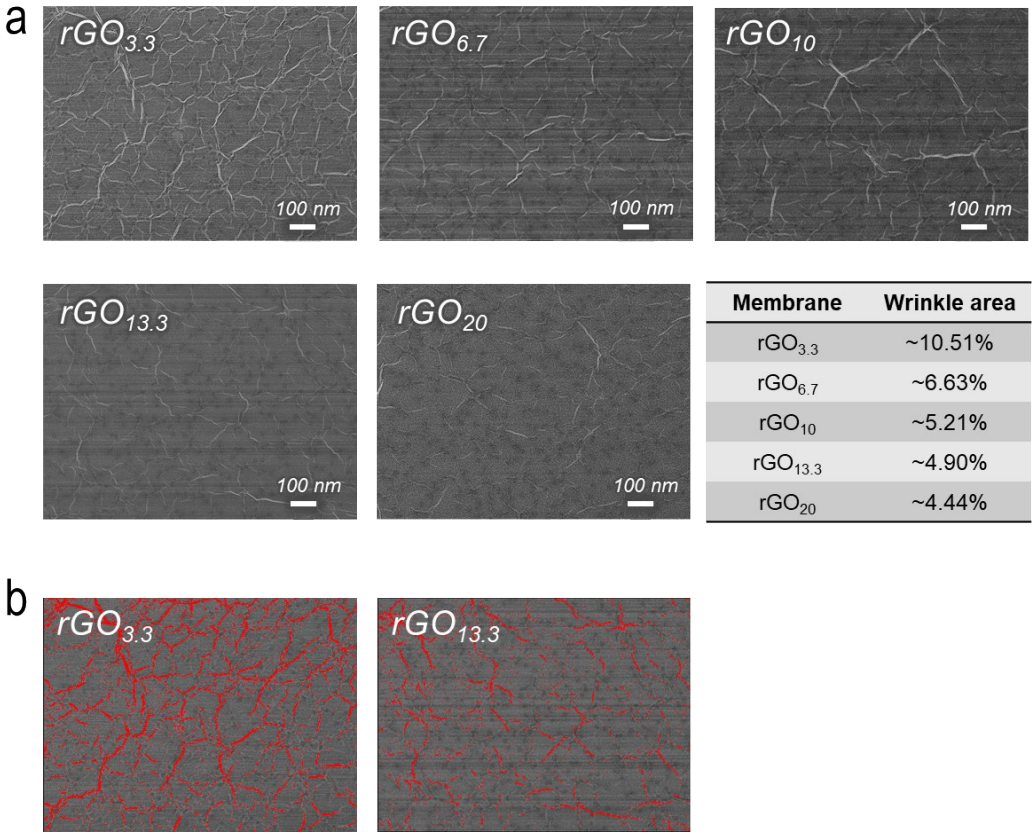

Membrane	Wrinkle area
$rGO_{3.3}$	~10.51%
$rGO_{6.7}$	~6.63%
rGO_{10}	~5.21%
$rGO_{13.3}$	~4.90%
rGO_{20}	~4.44%

Figure S9 a) SEM profiles of PC membrane filter-supported rGO membranes showing surface morphologies with wrinkles. b) SEM images of rGO membranes with wrinkles highlighted in red.

The percentage of the wrinkled area was obtained using ImageJ software. Taking $rGO_{3.3}$ and $rGO_{13.3}$ membranes as examples (Figure S9b), the wrinkles revealed in the SEM images could be recognized by the software. The percentage of the area was then estimated as the occupation of the highlighted pixels in the overall image.

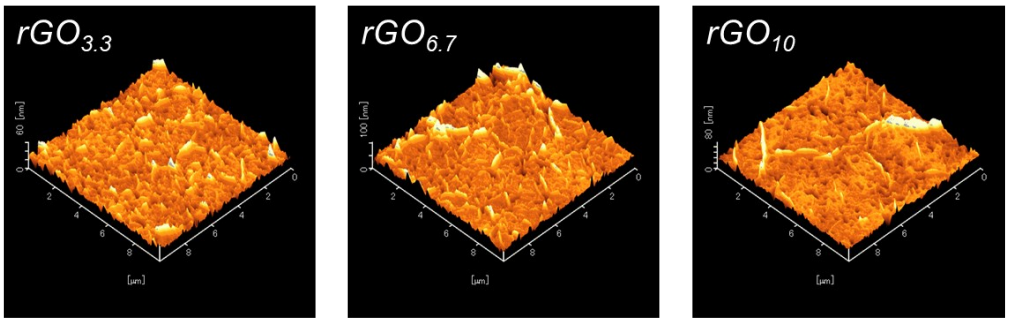

Membrane	R_a (nm)	R_{rms} (nm)
$rGO_{3.3}$	5.0 ± 0.7	7.1 ± 0.6
$rGO_{6.7}$	4.9 ± 1.8	6.9 ± 2.5
rGO_{10}	5.4 ± 0.5	7.8 ± 0.6
$rGO_{13.3}$	5.2 ± 0.7	7.7 ± 1.4
rGO_{20}	6.1 ± 1.7	7.0 ± 1.4

Figure S10 AFM images and corresponding roughness values for PC membrane filter-supported rGO membranes.

Although the morphologies of wrinkles from different rGO membranes varied, their overall surface roughness values were similar. This may imply that the roughness of the stacked rGO laminates was comparatively small compared to that of the substrates.

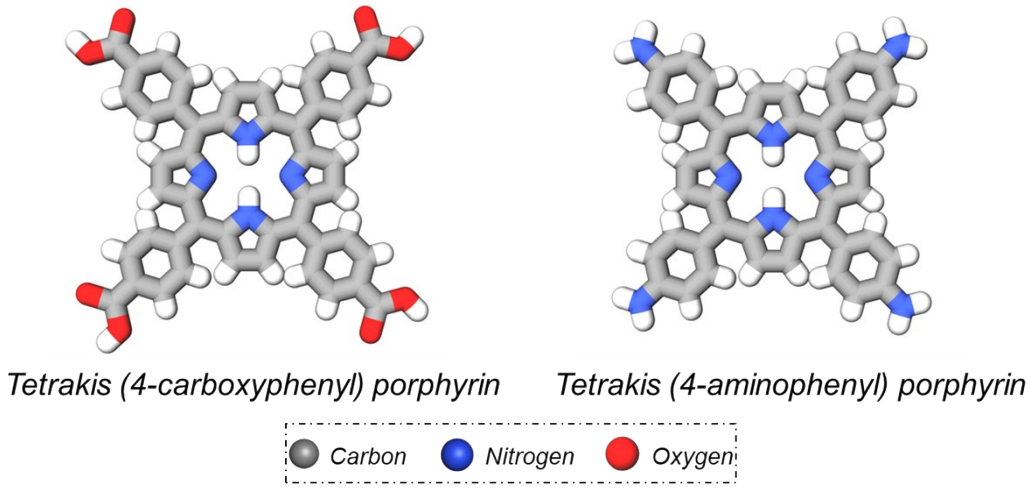

Figure S11 Molecular structures of two kinds of porphyrin-based chemicals.

Tetrakis(4-carboxyphenyl)porphyrin (TCPP) and tetrakis(4-aminophenyl)porphyrin (TAPP) comprise the negatively charged carboxyl and the positively charged amino groups, respectively.

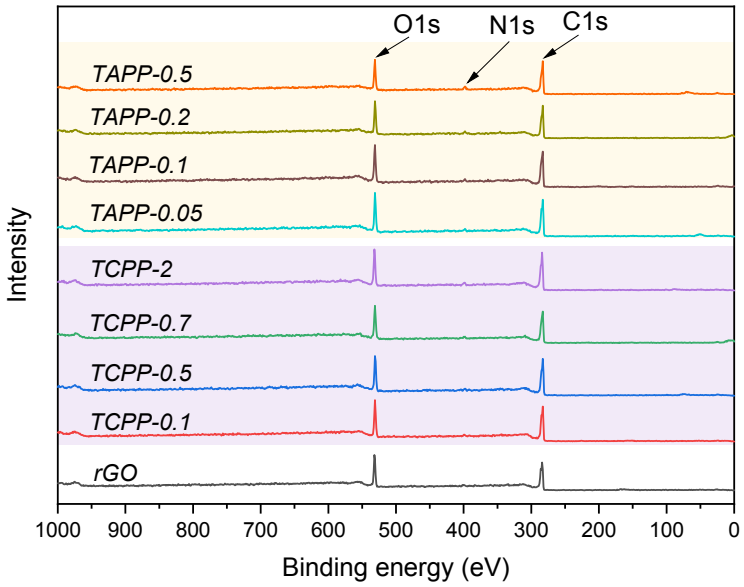

Figure S12 XPS survey spectra of porphyrin-functionalized rGO membranes.

The porphyrin-functionalized rGO membranes showed increased N1s peak intensity with higher dosages of porphyrins.

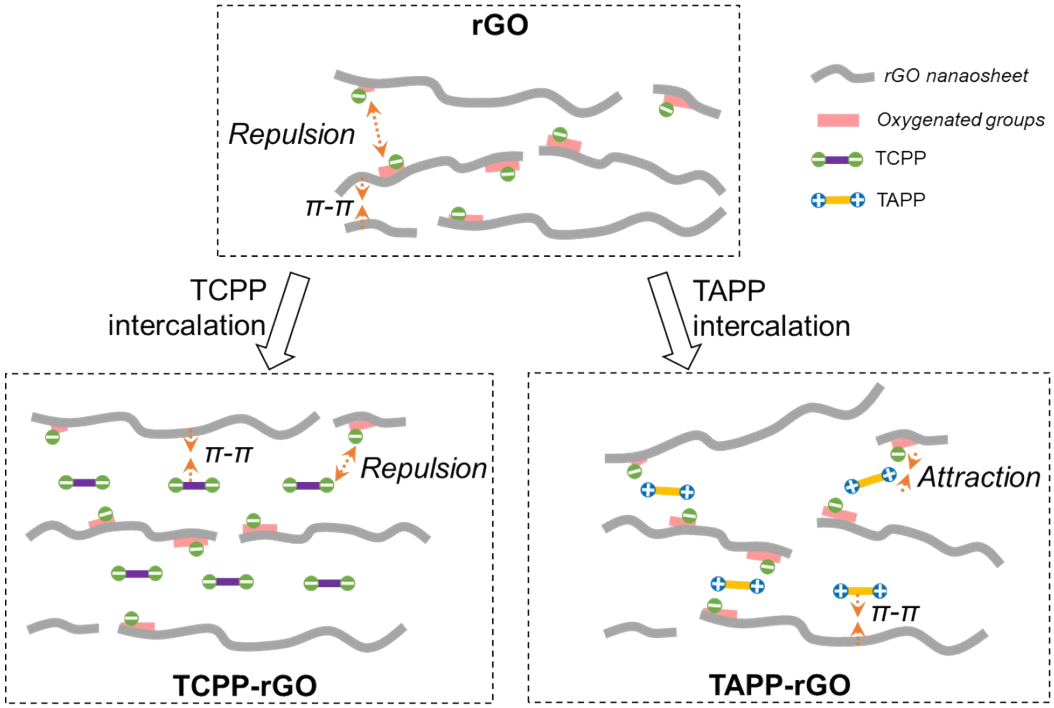

Figure S13 Illustration of the effects of TCPP and TAPP molecules in altering the structures of the rGO laminates.

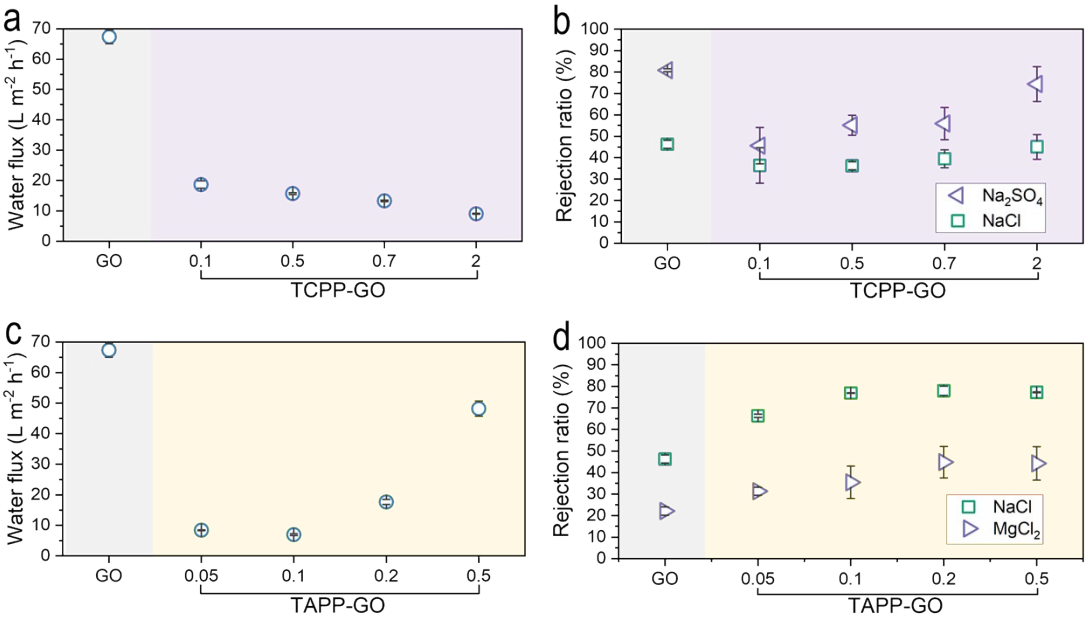

Figure S14 a, c) Water flux and b, d) salt rejection ratio of original GO, TCPP-GO, and TAPP-GO membranes. The dosage ratios of TCPP or TAPP to GO are shown in the figures.

When GO laminates were intercalated by porphyrin molecules, all the membranes showed worse salt rejection performances when compared to the corresponding intercalated rGO membranes. The higher intercalation amount of TAPP molecules results in a higher water flux while that of TCPP leads to a declined one. This could be explained by the interactions established between different porphyrin molecules and GO nanosheets that TAPP tends to disrupt the ordered stacking of GO while TCPP is more likely to render an ordered one. This structural evolution is similar to that of rGO membranes. The inclusion of more charged groups into the GO laminates contributes to the rejection of A_2B- or AB_2-type salts (TCPP for Na_2SO_4 and TAPP for $MgCl_2$), which is also confirmed by the intercalated rGO membranes. For TAPP-GO membranes, the cross-linking effect of TAPP helps to stabilize the membrane structure and give an increase of NaCl rejection; For TCPP-GO membranes, the repulsive force between TCPP and GO made the separation much worse. Although the π-π interaction between TCPP and GO is beneficial for the structural stability to some extent but not adequate to confine the nanochannel to retard ion transport. Therefore, TCPP-GO membranes exhibited even worse rejection performance than the original GO membrane. From performance results of GO and rGO based membranes, we may conclude that the stably confined nanochannel is a key factor to effectively reject ions and is also a prerequisite for further intercalation modifications to bring higher rejection ratios.

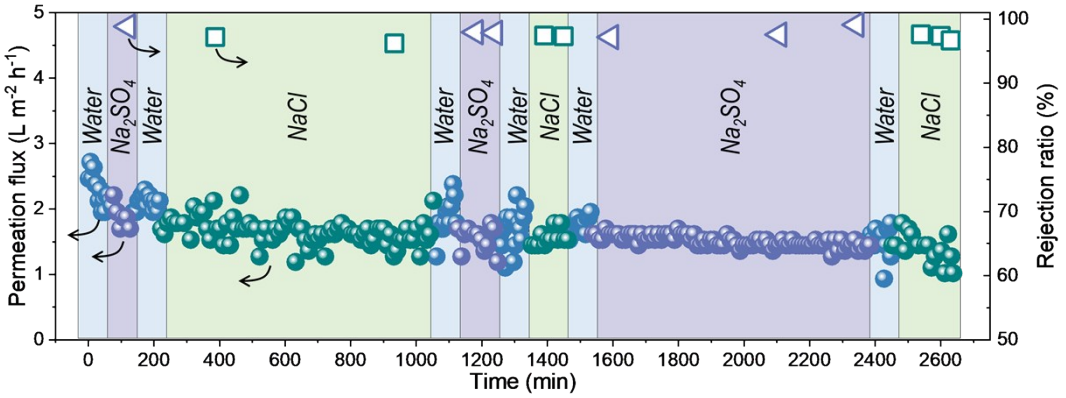

Figure S15 Sequential filtration of pure water, Na_2SO_4, pure water, and NaCl by a TCPP-rGO-0.7 membrane.

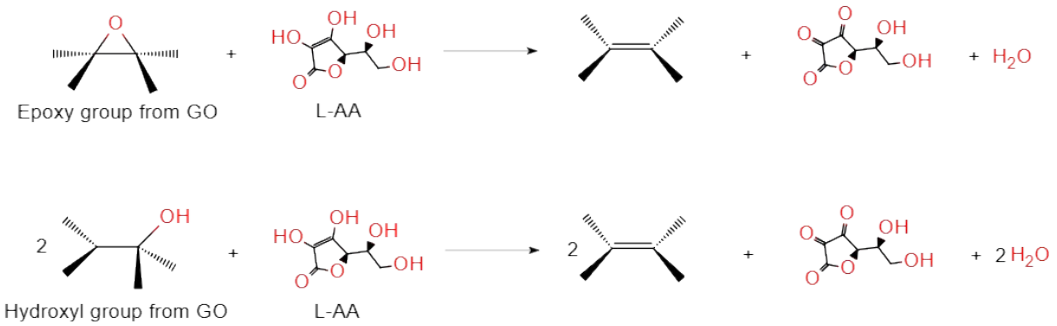

Figure S16 The reduction reactions of GO with L-AA.

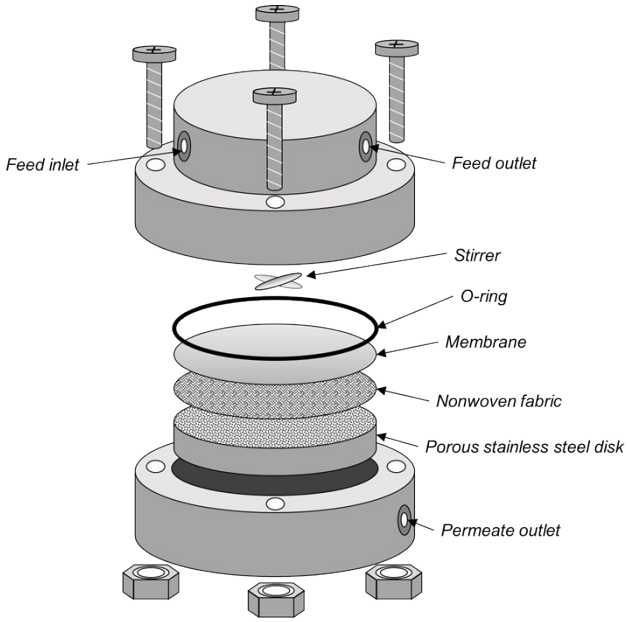

Figure S17 Components of the membrane cell used for the evaluation of desalination performance.

Table S1 Permeation flux and rejection ratio for different salts tested by the rGO membrane.

Salt type	Salt	Flux [L m^{-2} h^{-1}]	Rejection [%]
A_2B	Na_2SO_4	3.1 ± 0.4	98.1 ± 0.4
	K_2SO_4	2.5 ± 0.4	98.0 ± 0.6
AB	$MgSO_4$	1.4 ± 0.6	89.0 ± 2.1
	NaCl	2.7 ± 0.2	87.6 ± 2.0
	KCl	2.4 ± 0.7	82.3 ± 5.3
AB_2	$MgCl_2$	1.4 ± 0.6	52.7 ±10.3
	$CaCl_2$	1.4 ± 0.4	44.4 ± 5.4

Table S2 Permeation flux and rejection ratio for Na_2SO_4 and NaCl salts tested by the rGO and TCPP-rGO membrane.

Membrane	Water flux [L m^{-2} h^{-1}]	Na_2SO_4 rejection [%]	NaCl rejection [%]
rGO	2.9 ± 0.1	98.0 ± 0.3	87.6 ± 2.0
TCPP-rGO-0.1	5.4 ± 1.6	96.9 ± 1.7	77.2 ± 3.0
TCPP-rGO-0.2	2.6 ± 0.6	98.0 ± 0.7	89.2 ± 0.3
TCPP-rGO-0.7	1.7 ± 0.4	98.9 ± 0.3	92.2 ± 2.8
TCPP-rGO-2	1.2 ± 0.1	98.7 ± 0.2	92.8 ± 1.1

Table S3 Permeation flux and rejection ratio for $MgCl_2$ and NaCl salts tested by the rGO and TAPP-rGO membrane.

Membrane	Water flux [L m^{-2} h^{-1}]	$MgCl_2$ rejection [%]	NaCl rejection [%]
rGO	2.9 ± 0.1	52.7 ± 10.3	87.6 ± 2.0
TAPP-rGO-0.05	2.1 ± 1.0	59.6 ± 9.4	88.2 ± 4.2
TAPP-rGO-0.1	1.6 ± 0.6	57.7 ± 3.9	90.8 ± 2.3
TAPP-rGO-0.2	1.1 ± 0.4	68.1 ± 5.8	93.2 ± 2.2
TAPP-rGO-0.5	1.0 ± 0.4	65.5 ± 7.5	92.5 ± 0.6

Table S4 Interactions within rGO, TAPP-rGO, and TCPP-rGO membranes.

		rGO	rGO + TCPP	rGO + TAPP
Repulsive forces	Electrostatic repulsion *(carboxyl-carboxyl, rGO)*	✓	✓	✓
	Electrostatic repulsion *(carboxyl-carboxyl, rGO-TCPP)*	✘	✓	✘
Attractive forces	π-π interaction *(aromatic-aromatic, rGO)*	✓	✓	✓
	π-π interaction *(aromatic-aromatic, rGO-porphyrin)*	✘	✓	✓
	Electrostatic attraction *(carboxyl-amino, rGO-TAPP)*	✘	✘	✓

Table S5 Summary of literature reports on the NaCl rejection performance of GO-based membranes.

Membrane	Permeation flux [L m^{-2} h^{-1}]	Feed NaCl concentration [ppm]	NaCl rejection ratio [%]	Reference
GO-PEI	7	2000	55	S1
GO-COOH	4.9	2000	39	S2
GO-EDA-HPEI	5.5	1000	58	S3
GO-PEI	4.2	1000	38	S4
TA-GO-PEI	15	1000	64	S5
GO-TMC	102	1170	19	S6
brGO	16.3	1170	40	S7
GO/MWCNT	27.5	600	59	S8
PEI-GO/PAA/PVA/GA	4	N/A	43	S9
GO-graphene	17.3	2000	85	S10
GO	24	1000	35	S11
Holey GO	36.8	2000	40	S12
GO	71	2000	30	S13
GO	66.9	up to 5800	~0	S14
PEI/GO/PEI	21	1000	38	S15
PEI-GO	65.6	N/A	20	S16
GO	2	N/A	10	S17
rGO/CNT	84	300	42	S18
GO	4.5	2000	27	S19
GO	15	500	97	S20
Nanoporous rGO	240	1170	40	S21
GO	3.5	560	35	S22
BPPO/EDA/GO	3.14	1000	36	S23
GO/CN/TiO_2-CNT	32	2000	50	S24
PRGO/HNTs-PSS	35.2	N/A	7	S25
Graphene/SWNT	553	2000	85	S26
PE@ArGO	15	58.4	88	S27
GO-MoS_2	20	58.4	43	S28
rGO	33	500	42	S29
rGO	5	290	54	S30
GO	65.7	2000	64	S31
GO	38	584	52	S32
rGO	21	1000	~0	S33
GO-TEOA	6	N/A	30	S34
GO	30	100	20	S35
PES/GO/PES	40	500	60	S36
GO-TMPyP	10	2000	10	S37
GO-PEI	13.6	1750	20	S38

rGO	16	500	50	S39
GO-COF	120	1000	10	S40
rGO	2.8	58.4	65	S41
rGO	12	1000	50	S42
MoS_2/GO	50	1000	60	S43
GO	94	1000	25	S44
rGO	6.3	1000	83	S45
GO@Crown	12	400	60	S46

Table S6 Performance reproducibility of TCPP-rGO-0.7 membranes (applied pressure:10 bar; feed NaCl concentration: 500ppm).

TCPP-rGO-0.7 membrane No.	Water flux [L m^{-2} h^{-1}]	NaCl rejection [%]
1	1.4	94.2
2	2.0	90.2
3	1.6	96.7
4	1.2	94.3
5	1.6	96.2
6	1.2	93.7
7	1.1	93.1
8	0.8	96.3
Average	1.4	94.3

Supplementary references

S1. P. S. Parsamehr, M. Zahed, M. A. Tofighy, T. Mohammadi and M. Rezakazemi, *Desalination*, 2019, **468**, 114079.

S2. Y. Q. Yuan, X. L. Gao, Y. Wei, X. Y. Wang, J. Wang, Y. S. Zhang and C. J. Gao, *Desalination*, 2017, **405**, 29-39.

S3. Y. Zhang, S. Zhang and T. S. Chung, *Environ. Sci. Technol.*, 2015, **49**, 10235-10242.

S4. Z. Q. Jia and Y. Wang, *J. Mater. Chem. A*, 2015, **3**, 4405-4412.

S5. M. Y. Lim, Y. S. Choi, J. Kim, K. Kim, H. Shin, J. J. Kim, D. M. Shin and J. C. Lee, *J. Membr. Sci.*, 2017, **521**, 1-9.

S6. M. Hu and B. Mi, *Environ. Sci. Technol.*, 2013, **47**, 3715-3723.

S7. Y. Han, Z. Xu and C. Gao, *Adv. Funct. Mater.*, 2013, **23**, 3693-3700.

S8. Y. Han, Y. Jiang and C. Gao, *ACS Appl. Mater. Interfaces*, 2015, **7**, 8147-8155.

S9. N. X. Wang, S. L. Ji, G. J. Zhang, J. Li and L. Wang, *Chem. Eng. J.*, 2012, **213**, 318-329.

S10. A. Morelos-Gomez, R. Cruz-Silva, H. Muramatsu, J. Ortiz-Medina, T. Araki, T. Fukuyo, S. Tejima, K. Takeuchi, T. Hayashi, M. Terrones and M. Endo, *Nat. Nanotechnol.*, 2017, **12**, 1083-1088.

S11. R. Hu, G. Zhao, Y. He and H. Zhu, *Desalination*, 2020, **477**, 114271.

S12. X. Chen, Z. Feng, J. Gohil, C. M. Stafford, N. Dai, L. Huang and H. Lin, *ACS Appl. Mater. Interfaces*, 2020, **12**, 1387-1394.

S13. A. Akbari, P. Sheath, S. T. Martin, D. B. Shinde, M. Shaibani, P. C. Banerjee, R. Tkacz, D. Bhattacharyya and M. Majumder, *Nat. commun.*, 2016, **7**, 10891.

S14. H. Huang, Y. Mao, Y. Ying, Y. Liu, L. Sun and X. Peng, *Chem. Commun.*, 2013, **49**, 5963-5965.

S15. Q. Nan, P. Li and B. Cao, *Appl. Surf. Sci.*, 2016, **387**, 521-528.

S16. T. Wang, J. R. Lu, L. L. Mao and Z. N. Wang, *J. Membr. Sci.*, 2016, **515**, 125-133.

S17. J. Wang, P. Zhang, B. Liang, Y. Liu, T. Xu, L. Wang, B. Cao and K. Pan, *ACS Appl. Mater. Interfaces*, 2016, **8**, 6211-6218.

S18. X. Chen, M. Qiu, H. Ding, K. Fu and Y. Fan, *Nanoscale*, 2016, **8**, 5696-5705.

S19. F. Baskoro, C. B. Wong, S. R. Kumar, C. W. Chang, C. H. Chen, D. W. Chen and S. J. Lue, *J. Membr. Sci.*, 2018, **554**, 253-263.

S20. W. Li, W. Wu and Z. Li, *ACS Nano*, 2018, **12**, 9309-9317.

S21. Y. Li, W. Zhao, M. Weyland, S. Yuan, Y. Xia, H. Liu, M. Jian, J. Yang, C. D. Easton, C. Selomulya and X. Zhang, *Environ. Sci. Technol.*, 2019, **53**, 8314-8323.

S22. G. G. Liu, H. Q. Ye, A. T. Li, C. Y. Zhu, H. Jiang, Y. Liu, K. Han and Y. H. Zhou, *Carbon*, 2016, **110**, 56-61.

S23. N. Meng, W. Zhao, E. Shamsaei, G. Wang, X. K. Zeng, X. C. Lin, T. W. Xu, H. T. Wang and X. W. Zhang, *J. Membr. Sci.*, 2018, **548**, 363-371.

S24. Q. Zhang, S. Chen, X. F. Fan, H. G. Zhang, H. T. Yu and X. Quan, *Appl. Catal. B-Environ.*, 2018, **224**, 204-213.

S25. L. P. Zhu, H. X. Wang, J. Bai, J. D. Liu and Y. T. Zhang, *Desalination*, 2017, **420**, 145-157.

S26. Y. Yang, X. Yang, L. Liang, Y. Gao, H. Cheng, X. Li, M. Zou, R. Ma, Q. Yuan and X. Duan, *Science*, 2019, **364**, 1057-1062.

S27. X. Song, R. S. Zambare, S. Qi, B. N. Sowrirajalu, A. P. James Selvaraj, C. Y. Tang and C. Gao, *ACS Appl. Mater. Interfaces*, 2017, **9**, 41482-41495.

S28. P. Zhang, J. L. Gong, G. M. Zeng, B. Song, W. C. Cao, H. Y. Liu, S. Y. Huan and P. Peng, *J. Membr. Sci.*, 2019, **574**, 112-123.

S29. Z. Zhang, N. Li, Y. Sun, H. Yang, X. Zhang, Y. Li, G. Wang, J. Zhou, L. Zou and Z. Hao, *ACS Appl. Mater. Interfaces*, 2018, **10**, 27205-27214.

S30. Y. H. Chang, Y. D. Shen, D. B. Kong, J. Ning, Z. C. Xiao, J. X. Liang and L. J. Zhi, *RSC Adv.*, 2017, **7**, 2544-2549.

S31. H. Khorramdel, E. Dabiri, F. F. Tabrizi and M. Galehdari, *Sep. Purif. Technol.*, 2019, **212**, 497-504.

S32. Y. Lyu, Q. Q. Zhang, Z. X. Wang and J. W. Pu, *BioResources*, 2018, **13**, 9116-9131.

S33. Z. Y. Zhao, S. N. Ni, X. Su, Y. Gao and X. Q. Sun, *ACS Sustain. Chem. Eng.*, 2019, **7**, 14874-14882.

S34. K. Nakagawa, S. Araya, M. Kunimatsu, T. Yoshioka, T. Shintani, E. Kamio and H. Matsuyama, *Membranes (Basel)*, 2018, **8**, 130.

S35. Q. M. Wang, G. J. Zhao, C. X. Li and H. Meng, *J. Membr. Sci.*, 2019, **586**, 177-184.

S36. W. F. Wu, J. Y. Su, M. M. Jia, W. M. Zhong, Z. J. Li and W. B. Li, *J. Mater. Chem. A*, 2019, **7**, 13007-13011.

S37. X. L. Xu, F. W. Lin, Y. Du, X. Zhang, J. Wu and Z. K. Xu, *ACS Appl. Mater. Interfaces*, 2016, **8**, 12588-12593.

S38. Y. Liu, S. X. Zheng, P. Gu, A. J. Ng, M. N. Wang, Y. Y. Wei, J. J. Urban and B.

X. Mi, *Carbon*, 2020, **160**, 219-227.

S39. Z. S. Zhang, L. D. Zou, C. Aubry, M. Jouiad and Z. P. Hao, *J. Membr. Sci.*, 2016, **515**, 204-211.

S40. X. K. Zhang, H. Li, J. Wang, D. L. Peng, J. D. Liu and Y. T. Zhang, *J. Membr. Sci.*, 2019, **581**, 321-330.

S41. P. Zhang, J.-L. Gong, G.-M. Zeng, B. Song, S. Fang, M. Zhang, H.-Y. Liu, S.-Y. Huan, P. Peng, Q.-Y. Niu, D.-B. Wang and J. Ye, *Sep. Purif. Technol.*, 2019, **220**, 309-319.

S42. Y. Li, S. Yuan, Y. Xia, W. Zhao, C. D. Easton, C. Selomulya and X. Zhang, *J. Membr. Sci.* 2020, **601**, 117900.

S43. J. Ma, X. D. Tang, Y. He, Y. Fan, J. Y. Chen and H. Yu, *Desalination*, 2020, **480**, 114328.

S44. S. Xue, C. Ji, M. D. Kowal, J. C. Molas, C. W. Lin, B. T. McVerry, C. L. Turner, W. H. Mak, M. Anderson, M. Muni, E. M. V. Hoek, Z. L. Xu and R. B. Kaner, *Nano Lett.*, 2020, **20**, 2209-2218.

S45. S. Yuan, Y. Li, Y. Xia, Y. Kang, J. D. Yang, H. Uddin, H. Y. Liu, C. Selomulya and X. W. Zhang, *Environ. Sci. Technol. Lett.*, 2020, **7**, 273-279.

S46. K. R. Bang, D. Bahamon, L. F. Vega and E. S. Cho, *Adv. Mater. Interfaces*, 2020, **7**, 1901876.